

Sharp increase in central Oklahoma seismicity since 2008 induced by massive wastewater injection

K. M. Keranen,^{1*} M. Weingarten,² G. A. Abers,^{3†} B. A. Bekins,⁴ S. Ge²

¹Department of Earth and Atmospheric Sciences, Cornell University, Ithaca, NY, USA. ²Department of Geological Sciences, University of Colorado, Boulder, CO, USA. ³Lamont-Doherty Earth Observatory of Columbia University, Palisades, NY, USA. ⁴U.S. Geological Survey, Menlo Park, CA, USA.

*Corresponding author. E-mail: keranen@cornell.edu

†Present address: Department of Earth and Atmospheric Sciences, Cornell University, Ithaca, NY, USA.

Unconventional oil and gas production provides a rapidly growing energy source; however, high-production states in the United States, such as Oklahoma, face sharply rising numbers of earthquakes. Subsurface pressure data required to unequivocally link earthquakes to injection are rarely accessible. Here we use seismicity and hydrogeological models to show that fluid migration from high-rate disposal wells in Oklahoma is potentially responsible for the largest swarm. Earthquake hypocenters occur within disposal formations and upper-basement, between 2–5 km depth. The modeled fluid pressure perturbation propagates throughout the same depth range and tracks earthquakes to distances of 35 km, with a triggering threshold of ~0.07 MPa. Although thousands of disposal wells operate aseismically, four of the highest-rate wells are capable of inducing 20% of 2008–2013 central US seismicity.

Seismicity in the United States midcontinent surged beginning in 2008 (1), predominantly within regions of active unconventional hydrocarbon production (2–6). In Arkansas, Texas, Ohio, and near Prague, Oklahoma, recent earthquakes have been linked to wastewater injection (2–7) although alternative interpretations have been proposed (1, 8). Conclusively distinguishing human-induced earthquakes based solely on seismological data remains challenging..

Seismic swarms within Oklahoma dominate the recent seismicity in the central and eastern United States (9), contributing 45% of M3 and larger earthquakes between 2008–2013 (10). No other state contributed more than 11%. A single swarm, beginning in 2008 near Jones, Oklahoma, accounts for 20% of seismicity in this region (10). East of Jones, the damaging 2011 $M_{w}5.7$ earthquake near Prague, Oklahoma was likely induced by wastewater injection (2, 8, 11, 12), the highest magnitude to date. These earthquakes are part of a 40-fold increase in seismicity within Oklahoma during 2008–2013 as compared to 1976–2007 (Fig. 1, inset A) (10). Wastewater disposal volumes have also increased rapidly, nearly doubling in central Oklahoma between 2004–2008. Many studies of seismicity near disposal wells rely upon statistical relationships between the relative timing of seismicity, disposal well location, and injected water volume to evaluate a possible causal relationship (3–7, 13).

Here we focused on the Jones swarm and compared modeled pore pressure from hydrogeological models to the best-constrained earthquake hypocenters (14). Using data from local U. S. Geological Survey NetQuake accelerometers, the Earthscope Transportable Array and a small local seismic network (fig. S1), we generated a catalog of well-located earthquakes between 2010–2013. Event-station distances were predominantly less than 10 km (fig. S2d) and all earthquakes were recorded on at least one seismometer within 20 km of the initial hypocenter. To study pore pressure changes at earthquake hypocenters and the apparent migration in seismicity, we developed a three-dimensional hydro-

geological model of pore pressure diffusion from injection wells.

The Jones swarm began within 20 km of high-rate wastewater disposal wells, among the highest rate in Oklahoma, between two regions of fluid injection (Fig. 2). The four high-rate wells are southwest of Jones in southeast Oklahoma City (SE OKC) and dispose of ~4 million barrels/month (15) (Fig. 3). The target injection depth is 2.2–3.5 km into the Cambrian-Ordovician Arbuckle Group (fig. S3), a dolomitized carbonate; one disposal well ends near Precambrian basement. The large disposal wells are within dewatering plays (fig. S4). Dewatering production wells produce substantial wastewater volumes with initially up to 200 times greater water per barrel of oil than conventional production wells (16, 17). The rate of wastewater disposal in central Oklahoma has gradually increased since the mid-1990s (fig. S5), but disposal rates jumped after 2004 as high-rate injection wells began operating, including the first of the SE OKC wells in 2005 (Fig. 3) (15). Seismic moment release escalated in the Jones swarm in 2009, concurrent with the initial reported application of positive wellhead pressure at the SE OKC wells

(Fig. 3B).

Earthquakes in our catalog primarily nucleated within either the Arbuckle Group or within the upper 2 km of basement, with 22–33% above basement (Fig. 2B, fig. S6). Well-constrained earthquake hypocenters from March to October 2010 migrated northeast from the initial swarm centroid near Jones at 0.1–0.15 km/day (Fig. 2C–D), followed by a broad spread in seismicity. Earthquake hypocenters are not diffusely distributed; instead, relocated aftershock sequences of individual earthquakes (18) illuminate narrow faults parallel to one plane of calculated focal mechanisms (19) (Fig. 2A, insets). An earthquake on August 2, 2010, ruptured a portion of a 7-km-long mapped fault; if the entire fault had ruptured earthquake scaling laws suggest a maximum magnitude of $\sim M_6.0$ (20). Earthquakes later in 2010 ruptured an unmapped east-southeast to west-northwest trending fault, at an oblique angle to the overall northeast-southwest migration direction of the swarm. Although the swarm of seismicity migrates to the northeast parallel to structural dip, the individual faults, as evidenced by earthquake lineations, are not preferentially oriented in this direction.

Our hydrogeological model simulated injection into the Arbuckle Group using reported injection rates at 89 wells within 50 km of the Jones swarm between 1995–2012 (14). The wells include the four high-rate wells in SE OKC and 85 wells to the northeast of Jones. The model predicts a region of high fluid pressure perturbation spreading radially eastward from the SE OKC wells, and a lesser perturbation around the lower-rate wells to the northeast (Fig. 4). The high pore pressure increase occurs within the Arbuckle Group and in the upper 1–2 km of the basement in our model; nearly all earthquakes occur within this same depth range (Fig. 2B). The migrating front of the Jones earthquake swarm corresponds closely to the expanding modeled pressure perturbation away from the SE OKC wells, which reaches 25 km from the wells by December 2009 and to ~35 km by December 2012. The pore pressure

change modeled at each hypocenter indicates a critical threshold of ~ 0.07 MPa, above which earthquakes are triggered. This threshold is compatible with prior observations that static stress changes of as little as $\sim 0.01\text{--}0.1$ MPa are sufficient to trigger earthquakes when faults are near failure in the ambient stress field (21–23).

Our results indicate that, for modeled diffusivities, $\sim 85\%$ of the pore pressure perturbation is contributed by the four high-rate SE OKC wells. The 85 wells to the northeast contribute $\sim 15\%$ additional pore pressure change at the center of the Jones swarm by the end of 2012, and may contribute to the triggering of earthquakes particularly outside the region affected by the SE OKC wells (fig. S7). The modeled dominance of the SE OKC wells is attributable to their high rate; these wells include one of the largest wells in the state and three closely spaced wells 3.5 km away with a combined monthly volume of ~ 3 million barrels/month. The only other Oklahoma wells of similar size, in northern Oklahoma (fig. S8), are on the boundary of a second rapidly growing seismic swarm (Fig. 1). The summed rate of this well cluster near SE OKC is higher than previous cases of reported induced seismicity (Fig. 3a), including several times higher than the high-rate disposal wells linked to earthquakes near Dallas-Fort Worth, Texas and Cleburne, Texas (5–7). Comprehensive compilations of injection well rates for other high-injection states, including Texas and California, are not yet accessible.

We view the expanding Jones earthquake swarm as a response to regionally increased pore pressure from fluids primarily injected at the SE OKC wells. As the pressure perturbation expanded and encountered faults at various orientations, critically stressed, optimally oriented faults are expected to rupture first (24). Additional faults at near optimal orientations may rupture following further pressure increase (Fig. 4). As fluid pressure continues to propagate away from the wells and disturbs a larger and larger volume, the probability increases that fluid pressure will encounter a larger fault and induce a larger magnitude earthquake. The absence of earthquakes in regions above the critical pressure threshold may result from either a lack of faults or lack of well-oriented, critically-stressed faults. Alternatively, fluid flow may preferentially migrate along bedding structure (Fig. 2a).

Though seven earthquakes were recorded in 2006–2009 near the base of the SE OKC wellbores (10), the main swarm began ~ 15 km to the northeast (fig. S9), despite the high modeled pressure perturbation near the wells. Earthquakes in 2009 primarily occurred, within location uncertainty, near injection wells or on the nearest known faults to the northeast of the wells (fig. S9). Focal mechanisms near the swarm onset indicate fault planes at orientations favorable to failure (19, Fig. 2, inset B). Faults subparallel to the NNW-SSE-trending Nemaha fault would not be well-oriented for failure in the regional $\sim N70E$ stress regime (25) and would require substantially larger pressure increase to fail. Recent earthquakes near the fault may be evidence for continued pressure increase. This 50-km-long segment of the Nemaha fault is capable of hosting a M7 earthquake based on earthquake scaling laws (20) and the fault zone continues for hundreds of kilometers. The increasing proximity of the earthquake swarm to the Nemaha fault presents a potential hazard for the Oklahoma City metropolitan area.

Our earthquake relocations and pore pressure models indicate that four high-rate disposal wells are capable of increasing pore pressure above the reported triggering threshold (21–23) throughout the Jones swarm, and thus are capable of triggering $\sim 20\%$ of 2008–2013 central and eastern US seismicity. Nearly 45% of this region's seismicity, and currently nearly 15 M >3 earthquakes per week, may be linked to disposal of fluids generated during Oklahoma dewatering and following hydraulic-fracturing, as recent Oklahoma seismicity dominantly occurs within seismic swarms in the Arbuckle Group, Hunton Group, and Mississippi Lime dewatering plays. The injection-linked seismicity near Jones occurs up to 35 km away from the disposal wells, much further than previously considered in existing criteria for induced seismicity

(13). Modern, very high-rate injection wells can therefore impact regional seismicity and increase seismic hazard. Regular measurements of reservoir pressure at a range of distances and azimuths from high-rate disposal wells could verify our model and potentially provide early indication of seismic vulnerability.

References and Notes

1. W. L. Ellsworth, *W.L. Science* **341**, 1225942 (2013).
2. K. Keranen, H. Savage, G. Abers, E. Cochran, Potentially induced earthquakes in Oklahoma, USA: Links between wastewater injection and the 2011 M_w 5.7 earthquake. *Geology* **41**, 699–702 (2013). doi:[10.1130/G34045.1](https://doi.org/10.1130/G34045.1)
3. W.-Y. Kim, *J. Geophys. Res.* **118**, 3506–3518 (2013).
4. S. Horton, Disposal of hydrofracking waste fluid by injection into subsurface aquifers triggers earthquake swarm in central Arkansas with potential for damaging earthquake. *Seismol. Res. Lett.* **83**, 250–260 (2012). doi:[10.1785/gssrl.83.2.250](https://doi.org/10.1785/gssrl.83.2.250)
5. C. Frohlich, C. Hayward, B. Stump, E. Potter, The Dallas-Fort Worth Earthquake Sequence: October 2008 through May 2009 *Bull. Seismol. Soc. Am.* **101**, 327–340 (2011). doi:[10.1785/0120100131](https://doi.org/10.1785/0120100131)
6. A. H. Justinic, B. Stump, C. Hayward, C. Frohlich, Analysis of the Cleburne, Texas, earthquake sequence from June 2009 to June 2010. *Bull. Seismol. Soc. Am.* **103**, 3083–3093 (2013). doi:[10.1785/0120120336](https://doi.org/10.1785/0120120336)
7. C. Frohlich, Two-year survey comparing earthquake activity and injection-well locations in the Barnett Shale, Texas. *Proc. Natl. Acad. Sci. U.S.A.* **109**, 13934–13938 (2012). doi:[10.1073/pnas.1207728109](https://doi.org/10.1073/pnas.1207728109)
8. A. McGarr, Maximum magnitude earthquakes induced by fluid injection. *J. Geophys. Res.* **119**, 1008–1019 (2014). doi:[10.1002/2013JB010597](https://doi.org/10.1002/2013JB010597)
9. The Central and Eastern United States is considered the portion of the contiguous United States east of 109° W.
10. ANSS catalog, United States Geological Survey, <http://earthquake.usgs.gov/earthquakes/search/>, accessed 4/1/2014.
11. N. J. van der Elst, H. M. Savage, K. M. Keranen, G. A. Abers, Enhanced remote earthquake triggering at fluid-injection sites in the midwestern United States. *Science* **341**, 164–167 (2013). Medline doi:[10.1126/science.1238948](https://doi.org/10.1126/science.1238948)
12. D. F. Sumy, E. S. Cochran, K. M. Keranen, M. Wei, G. A. Abers, Observations of static Coulomb stress triggering of the November 2011 M5.7 Oklahoma earthquake sequence. *J. Geophys. Res.* **119**, 1904–1923 (2014). doi:[10.1002/2013JB010612](https://doi.org/10.1002/2013JB010612)
13. S. D. Davis, C. Frohlich, *Seismol. Res. Lett.* **64**, 207–224 (1993).
14. Information on materials and methods is available on *Science* Online.
15. Oklahoma Corporation Commission Imaging Web Application, <http://imaging.occeweb.com/>
16. D. Chernicky, *World Oil* (2000).
17. K. E. Murray, State-scale perspective on water use and production associated with oil and gas operations, Oklahoma, U.S. *Environ. Sci. Technol.* **47**, 4918–4925 (2013). Medline doi:[10.1021/es4000593](https://doi.org/10.1021/es4000593)
18. F. Waldhauser, W. L. Ellsworth, A Double-difference earthquake location algorithm: Method and application to the Northern Hayward Fault, California. *Bull. Seismol. Soc. Am.* **90**, 1353–1368 (2000). doi:[10.1785/0120000006](https://doi.org/10.1785/0120000006)
19. A. A. Holland, Optimal fault orientations within Oklahoma. *Seismol. Res. Lett.* **84**, 876–890 (2013). doi:[10.1785/0220120153](https://doi.org/10.1785/0220120153)
20. D. L. Wells, K. J. Coppersmith, *Bull. Seismol. Soc. Am.* **84**, 974–1002 (1994).
21. P. A. Reasenberg, R. W. Simpson, Response of regional seismicity to the static stress change produced by the loma prieta earthquake. *Science* **255**, 1687–1690 (1992). Medline doi:[10.1126/science.255.5052.1687](https://doi.org/10.1126/science.255.5052.1687)
22. L. Seeber, J. G. Armbruster, Earthquakes as beacons of stress change. *Nature* **407**, 69–72 (2000). doi:[10.1038/35024055](https://doi.org/10.1038/35024055) Medline doi:[10.1038/35024055](https://doi.org/10.1038/35024055)
23. R. Stein, The role of stress transfer in earthquake occurrence. *Nature* **402**, 605–609 (1999). doi:[10.1038/45144](https://doi.org/10.1038/45144)
24. M. D. Zoback, J. Townend, B. Grollimund, Steady-state failure equilibrium and deformation of intraplate lithosphere. *Int. Geol. Rev.* **44**, 383–401 (2002). doi:[10.2747/0020-6814.44.5.383](https://doi.org/10.2747/0020-6814.44.5.383)
25. M. L. Zoback, First- and second-order patterns of stress in the lithosphere: The World Stress Map Project. *J. Geophys. Res.* **97**, 11703–11728 (1992). doi:[10.1029/92JB00132](https://doi.org/10.1029/92JB00132)
26. K. V. Luza, J. E. Lawson, *Oklahoma Geological Survey Spec. Pub.* **81-3**, 1–67 (1981).
27. S. P. Gay, *Shale Shaker* **54**, 39–49 (2003).
28. L. E. Gatewood, in *Geology of giant petroleum fields*, AAPG Memoir **14**, M.

- T. Halbouty, Ed. (American Association of Petroleum Geologists Tulsa, OK, 1970).
29. Monthly average volume was calculated using reported volumes for any month with nonzero volume (15). Injection rates over 90% larger than the median monthly value in a given year for each well were removed from calculations to remove data entry errors.
 30. E. Kissling, W. L. Ellsworth, D. Eberhart-Phillips, U. Kradolfer, Initial reference models in local earthquake tomography. *J. Geophys. Res.* **99**, 19635–19646 (1994). doi:[10.1029/93JB03138](https://doi.org/10.1029/93JB03138)
 31. V. Jambunathan, thesis, Univ. of Oklahoma (2008).
 32. T. Brocher, Empirical relations between elastic wavespeeds and density in the Earth's crust. *Bull. Seismol. Soc. Am.* **95**, 2081–2092 (2005). doi:[10.1785/0120050077](https://doi.org/10.1785/0120050077)
 33. A. W. Harbaugh, E. R. Banta, M. C. Hill, M. G. McDonald, *U.S. Geological Survey Open-File Report 00-92* (2000).
 34. M. G. McDonald, A. W. Harbaugh, *U.S. Geol. Survey Open-File Report 83-875* (1984).
 35. E. K. Franseen, A. P. Byrnes, in J. R. Derby, R. D. Fritz, S. A. Longacre, W. A. Morgan, C. A. Sternbach, Eds., *AAPG Memoir 98*, 1031–1047 (2012).
 36. B. C. Haimson, T. W. Doe, State of stress, permeability, and fractures in the Precambrian granite of northern Illinois. *J. Geophys. Res.* **88**, 7355–7371 (1983). doi:[10.1029/JB088iB09p07355](https://doi.org/10.1029/JB088iB09p07355)
 37. S. A. Shapiro, E. Rothert, V. Rath, J. Rindschwentner, Characterization of fluid transport properties of reservoirs using induced microseismicity. *Geophysics* **67**, 212–220 (2002).
 38. International Seismological Centre, *On-line Bulletin*, International Seismological Centre, Thatcham, UK, 2011; <http://www.isc.ac.uk>.
 39. J. H. Healy, W. W. Rubey, D. T. Griggs, C. B. Raleigh, The Denver Earthquakes. *Science* **161**, 1301–1310 (1968). Medline doi:[10.1126/science.161.3848.1301](https://doi.org/10.1126/science.161.3848.1301)
 40. J. Ake, K. Mahrer, D. O'Connell, L. Block, Deep-injection and closely monitored induced seismicity at Paradox Valley, Colorado. *Bull. Seismol. Soc. Am.* **95**, 664–683 (2005). doi:[10.1785/0120040072](https://doi.org/10.1785/0120040072)
 41. L. Seeber, J. G. Armbruster, W.-Y. Kim, A fluid-injection-triggered earthquake sequence in Ashtabula, Ohio: Implications for seismogenesis in stable continental regions. *Bull. Seismol. Soc. Am.* **94**, 76–87 (2004). doi:[10.1785/0120020091](https://doi.org/10.1785/0120020091)

Acknowledgments: This research benefited from discussion with E. Cochran, W. Ellsworth, and participants in a US Geological Survey (USGS) Powell Center Working Group on Understanding Fluid Injection Induced Seismicity (M.W., B.B., and S.G. are part of this group). C. Hogan identified many P- and S-phases. K.M.K was partially supported by USGS National Earthquake Hazards Reduction Program (NEHRP) grant G13AP00025, M.W. was partially supported by the USGS Powell Center grant G13AC00023, and G.A.A. was partially supported by NEHRP grant G13AP00024. This project used seismic data from EarthScope's Transportable Array, a facility funded by the National Science Foundation. Seismic waveforms are from the Incorporated Research Institutions for Seismology Data Management Center and the USGS CWB Query. Well data are from the Oklahoma Corporation Commission and the Oklahoma Geological Survey. Lists of wells and the local earthquake catalog are available as supplementary materials on *Science* Online.

Supplementary Materials

www.sciencemag.org/cgi/content/full/science.1255802/DC1

Materials and Methods

Figs. S1 to S10

Tables S1 to S9

References (30–41)

8 May 2014; accepted 24 June 2014

Published online 03 July 2014

10.1126/science.1255802

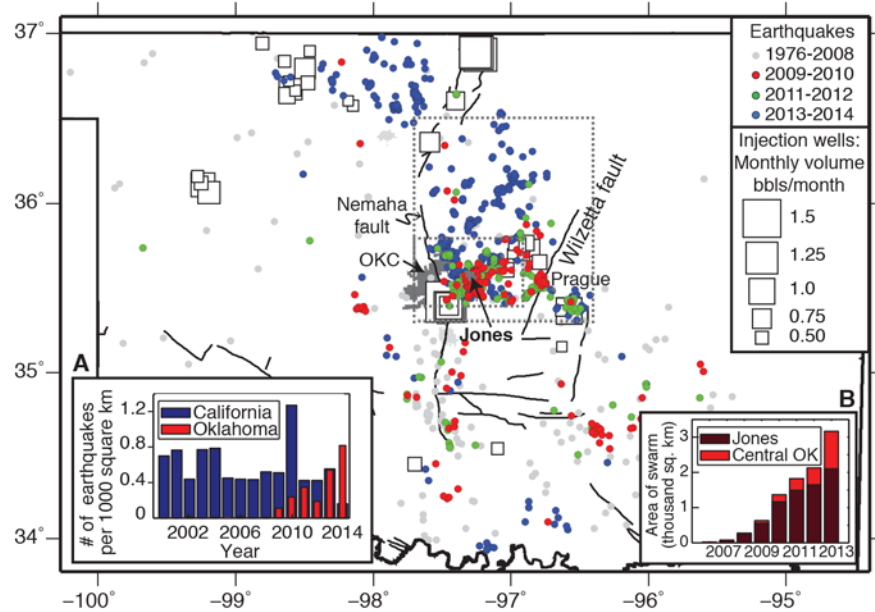


Fig. 1. Earthquakes in Oklahoma between 1976-2014. Earthquakes are magnitude > 1 from the NEIC catalog (10). Black lines are faults (26–28). Small and large dashed gray boxes outline the areas used for analysis of the Jones swarm and of central OK, respectively, in Inset B. OKC: Oklahoma City. Inset A: Comparison of M3+ earthquake rate in Oklahoma to California, normalized by area. California is ~2.3 times larger than Oklahoma. 2014 earthquakes are through the first four months. Inset B: Expanding area of the Jones and the broader central Oklahoma swarms. Regions were divided into 5x5 km grid cells and any cell with an earthquake was considered part of the swarm. Swarm area per year is inclusive of all prior years.

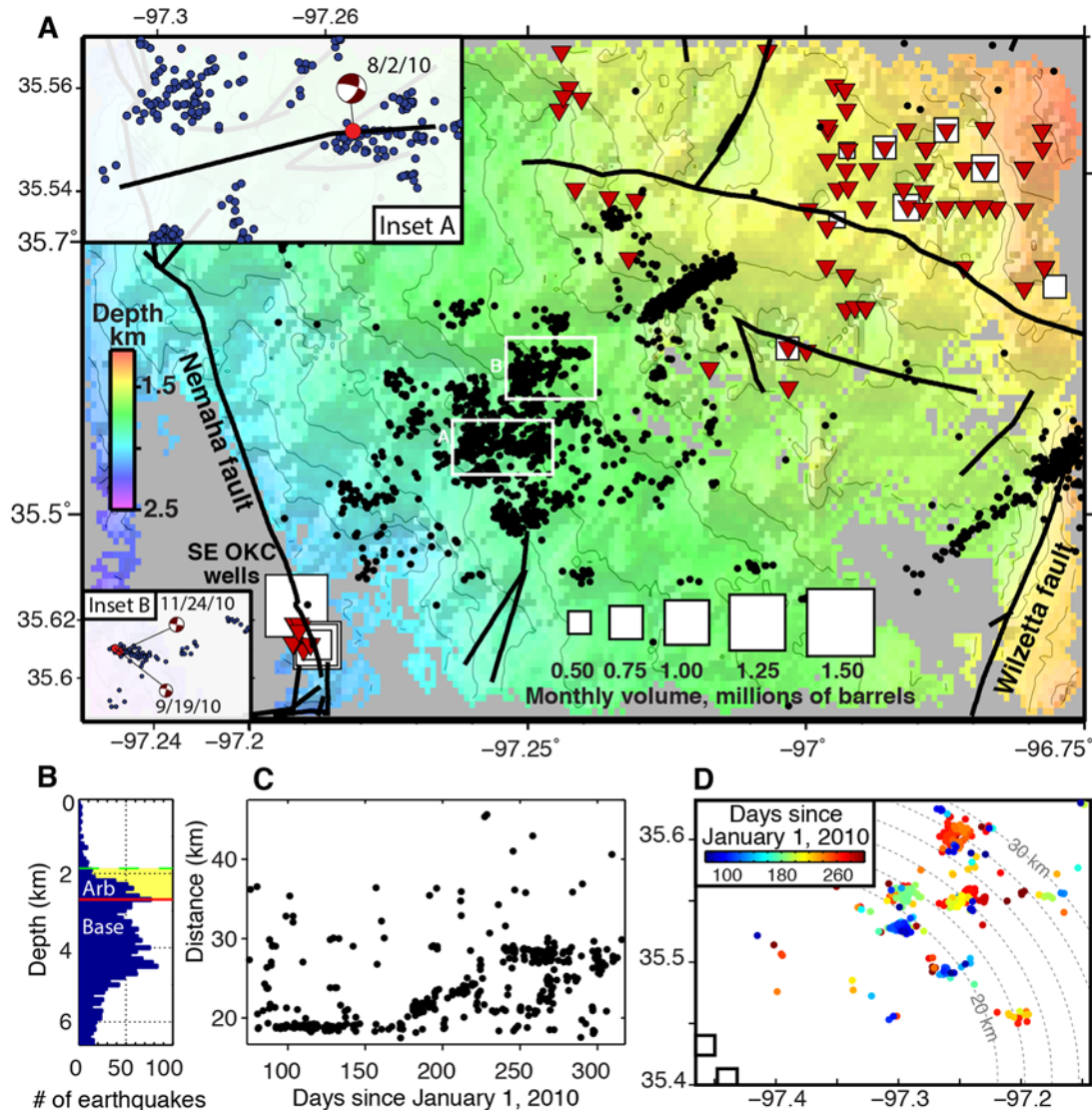


Fig. 2. Earthquake catalog and swarm migration. (A) Jones earthquake catalog March 2010–March 2013 using local stations. Squares are injection wells operating at an average rate $\geq 400,000$ barrels/month (15, 29), triangles are high-water-production wells. Background color and contours represent depth to the top of the Hunton Group (15). The Hunton Group is higher in section than the Arbuckle Group but has more data on formation depth. (B) Earthquake depth histogram; earthquakes are dominantly in sediment and upper basement. (C) Distance of each March–October 2010 Jones earthquake to the SE OKC disposal wells. The dense region of the swarm increases in distance between days 150 and 250 in 2010. (D) Map view of Jones earthquakes during March–October of 2010, colored by time. Semicircles are equidistant lines from SE OKC disposal wells. Faults at greater distance from the wells become active at later times. Details of two of these fault planes are shown in insets of Fig. 2A and are discussed in the text.

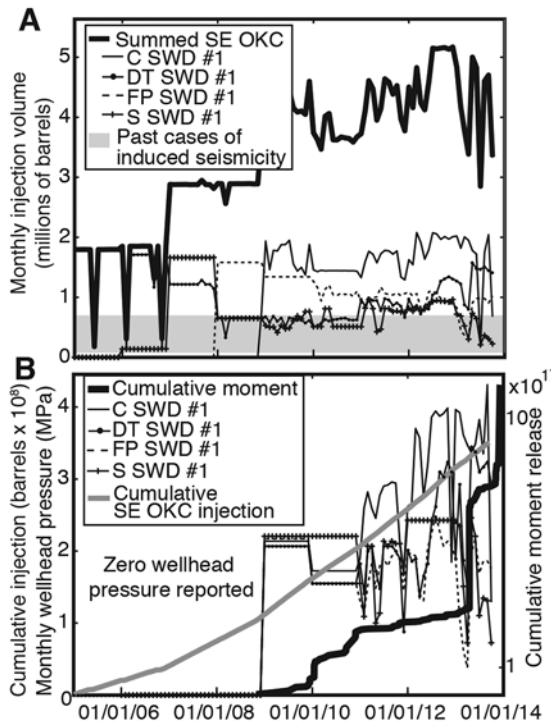


Fig. 3. Fluid injection reported in the four high-rate SE OKC wells. (A) Sum and individual monthly injection volumes and (B) wellhead pressure and cumulative, summed injected volume (15). The DT SWD #1, FP SWD #1, and S SWD #1 wells are in close proximity; the C SWD #1 well is ~3.5 km away. Gray shading denotes injection rates for notable past cases of induced seismicity for reference (table S1). Cumulative seismic moment in (B) is calculated from M3+ earthquakes from 2005 to January 2014 (10) for earthquakes within the box outlining the Jones swarm in Fig. 1.

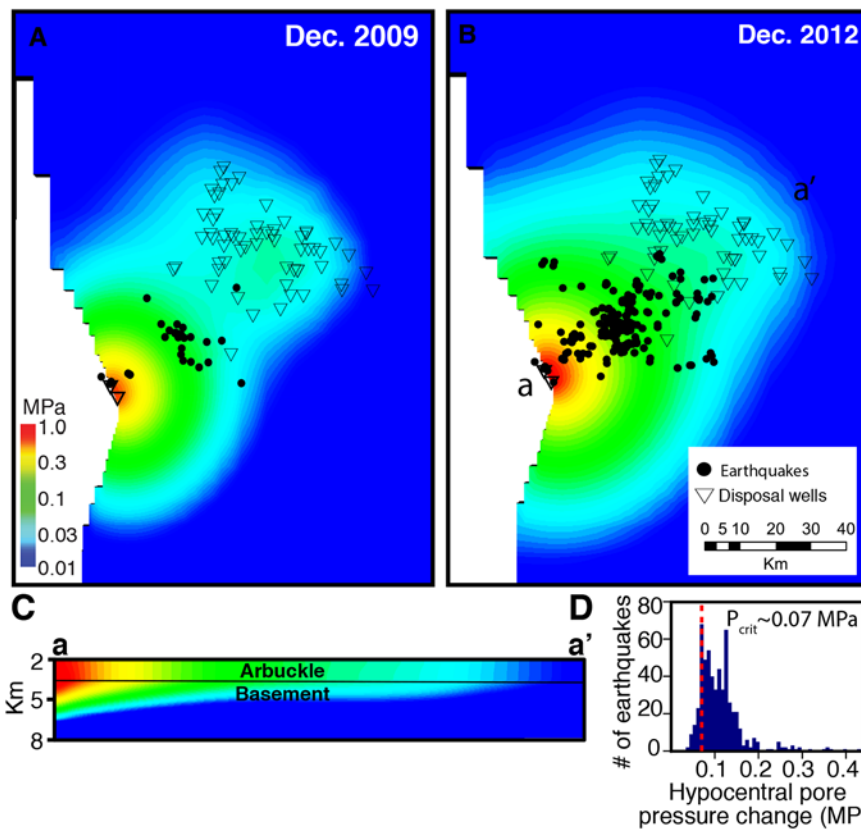


Fig. 4. Hydrogeologic model of pore pressure perturbation from injection wells. (A) Modeled pressure perturbation in December 2009 and (B) in December 2012 using a hydraulic diffusivity of $2 \text{ m}^2/\text{s}$ (14). The model includes the four high-rate SE OKC wells and 85 wells northeast of the Jones swarm near the West Carney field. The modeled pressure perturbation is dominated by fluid injected at the high-rate SE OKC wells. Earthquakes are plotted from 2008–2009 (A) and 2008–2012 (B) (10). (C) Vertical cross-section through model results. Pore pressure rises in the Arbuckle Group and uppermost basement. (D) Pore pressure increase at the hypocenter of each earthquake in our local catalog. A pore pressure increase of $\sim 0.07 \text{ MPa}$ is the modeled triggering threshold. Modeled pore pressure rises throughout much of the swarm area for hydraulic diffusivity between $1 \text{ m}^2/\text{s}$ and $4 \text{ m}^2/\text{s}$ (fig. S7).